

Maximum Likelihood Estimation of Delay and Phase for Chirped Signals

Victor Vilnrotter* and Julian Breidenthal*

ABSTRACT. — Chirped signals are well known in the context of bandwidth-efficient high-resolution radar, but their ability to provide accurate phase and delay calibration of antenna arrays has not been previously explored. Here we consider using chirped pulses to calibrate phased antenna arrays, for both transmit and receive applications. Array calibration requires the estimation of carrier phase and group delay, information that is inherently contained in a chirped signal pulse. In this article, we examine this new calibration capability by developing the structure of the maximum likelihood estimator, and simulating its performance over a wide range of signal-to-noise ratios (SNRs). The simulation results are compared to Cramer-Rao lower bounds on the variance of estimation error, for both individual and joint estimation of delay and phase. It is shown that chirped signals have the capability to provide accurate estimates of delay and phase with SNRs and integration times typically encountered in operational phased array applications.

I. Introduction

The Deep Space Network (DSN) is developing arrays of 34-m beam waveguide (BWG) antennas with the potential of eventually using them as an alternative to the existing 70-m antennas. One driver of this effort is lower cost per square meter of aperture for 34-m antennas compared to 70-m antennas. The question then arises, as to how 34-m antennas could be combined to provide a planetary radar capability comparable to the existing Goldstone Solar System Radar (GSSR) currently residing on the 70-m antenna at Goldstone, California. This radar transmits high power (100 kW to 500 kW) signals at X-band (8560 MHz), in various modes including continuous wave (CW), binary phase coded (BPC) modulation, as well as chirp modulation [1]. Its observations are used for planetary and asteroid studies, orbital debris studies, and recovery of lost or distressed spacecraft.

In the DSN, significant progress has been made in the development of phased uplink arrays [2, 3, 4]. The general strategy has been to transmit from multiple 34-m BWG antennas simultaneously, pre-calibrating the transmissions to produce constructive

* Communications Architectures and Research Section.

interference in the desired direction by illuminating a known target, and maximizing the arrayed signal power over the target to achieve phase calibration [2]. In various uplink array experiments, targets have included the Moon and the planets Mercury and Venus [3], as well as interplanetary spacecraft such as Extrasolar Planet Observation and Deep Impact Extended Investigation (EPOXI), the extended mission designation given to the Deep Impact spacecraft following its successful impactor mission to the comet Tempel 1 [4].

A key goal of arrayed transmission with N antennas is to achieve N^2 increase in effective isotropic radiated power (EIRP), with the potential of providing greatly increased EIRP at lower cost than can be obtained by increasing transmitter power of the existing single-antenna, as in the 70-m GSSR system. Such an increase in EIRP would be valuable for detection of smaller and more-distant radar targets, as well as high data rate communication with distant spacecraft. In all of these cases, estimation of signal parameters such as time delay and phase offset, and the dependence of the quality of those estimates on the SNR, is important. Here we discuss the joint estimation of time delay and phase for the particular case of chirp-modulated radar signals, commonly used in planetary radar due to their efficient use of bandwidth and ability to provide comprehensive information needed for rapid calibration of antenna arrays.

II. Maximum Likelihood Estimation of Signal and Noise Parameters

Following downconversion to complex baseband, the received signal at each antenna can be modeled as an N dimensional vector of complex time samples taken at integer multiples of the sampling interval Δt . The received samples can be represented as

$\tilde{r}(i\Delta t) = \tilde{s}(i\Delta t) + \tilde{n}(i\Delta t)$, where “ \sim ” denotes “complex.” Although important in deriving the signal model and noise statistics, the sampling interval Δt will be assumed to be known in the subsequent analysis and hence can be suppressed, yielding the simpler representation $\tilde{r}_i = \tilde{s}_i + \tilde{n}_i$, where the variance of the complex noise samples is σ_n^2 with independent zero-

mean Gaussian real and imaginary components, each with identical variance $\sigma^2 = \sigma_n^2 / 2$.

The vector of N received samples can now be conveniently represented in terms of signal and noise components as $\tilde{\mathbf{r}} = (\tilde{r}_1, \tilde{r}_2, \dots, \tilde{r}_N)$, $\tilde{\mathbf{s}} = (\tilde{s}_1, \tilde{s}_2, \dots, \tilde{s}_N)$, $\tilde{\mathbf{n}} = (\tilde{n}_1, \tilde{n}_2, \dots, \tilde{n}_N)$.

The chirp signal can be expressed as $\tilde{s}_i = A \exp\{j[\frac{1}{2}k_c(t_i - \tau)^2 + \theta]\}$, $t_i = i\Delta t$, where A is the signal amplitude. The noise variance σ_n^2 and the signal amplitude A are assumed to be known with the desired accuracy from previous measurements. The chirp rate parameter k_c , in units of radians/sample, is generated by the transmitter electronics and hence is also known. The unknown delay τ and the unknown carrier phase θ are the remaining parameters to be estimated in this article.

For independent noise samples, the joint probability density of the complex noise vector is the product of the individual noise densities, here assumed to be complex Gaussian:

$$p(\tilde{\mathbf{n}}) = (\pi \sigma_n^2)^{-N} \prod_{i=1}^N \exp(-|\tilde{n}_i|^2 / \sigma_n^2). \quad (1)$$

Given the signal parameter vector $\boldsymbol{\psi} = (\theta, \tau)$, the joint probability density of the received vector, conditioned on the phase θ and delay τ , can be expressed as:

$$p(\tilde{\mathbf{r}} | \boldsymbol{\psi}) = (\pi \sigma_n^2)^{-N} \prod_{i=1}^N \exp(-|\tilde{r}_i - \tilde{s}_i|^2 / \sigma_n^2). \quad (2)$$

The maximum likelihood (ML) estimates of the parameters are those values that simultaneously maximize the conditional joint probability density in Equation 2, or equivalently its natural logarithm, known as the “conditional log-likelihood function” $\Lambda(\tilde{\mathbf{r}} | \boldsymbol{\psi})$:

$$\Lambda(\tilde{\mathbf{r}} | \boldsymbol{\psi}) \equiv \ln[p(\tilde{\mathbf{r}} | \boldsymbol{\psi})] = -N \ln(\pi \sigma_n^2) + \frac{2}{\sigma_n^2} \operatorname{Re} \left(\sum_{i=1}^N \tilde{r}_i \tilde{s}_i^* \right) - \frac{1}{\sigma_n^2} \sum_{i=1}^N |\tilde{s}_i|^2 - \frac{1}{\sigma_n^2} \sum_{i=1}^N |\tilde{r}_i|^2. \quad (3)$$

Substituting $\tilde{s}_i^* = A \exp[-j(\frac{1}{2} k_c (t_i - \tau)^2 + \theta)]$ for the locally generated conjugate signal samples and recognizing that $|\tilde{s}_i|^2 = A^2$, we obtain

$$\Lambda(\tilde{\mathbf{r}} | \boldsymbol{\psi}) = -N \ln(\pi \sigma_n^2) + \frac{2A}{\sigma_n^2} \operatorname{Re} \left(\exp(-j\theta) \sum_{i=1}^N \tilde{r}_i \exp[-j\frac{1}{2} k_c (t_i - \tau)^2] \right) - \frac{NA^2}{\sigma_n^2} - \frac{1}{\sigma_n^2} \sum_{i=1}^N |\tilde{r}_i|^2.$$

Since we are only interested in estimating the phase θ and the delay τ , terms that do not contain these parameters in Equation 3 cannot contribute to the maximization, hence will be ignored. Equation 3 can now be rewritten in simplified form as

$$\Lambda_0(\tilde{\mathbf{r}} | \boldsymbol{\psi}) = \operatorname{Re} \left(\exp(-j\theta) \sum_{i=1}^N \tilde{r}_i \exp[-j\frac{1}{2} k_c (t_i - \tau)^2] \right). \quad (4)$$

First consider the estimation of the phase, θ . We recall that for any complex number \tilde{z} , the expression $\operatorname{Re}\{\tilde{z} \exp(-j\theta)\}$ is maximized with respect to θ when we let $\theta = \arg(\tilde{z})$,

attaining its maximum value $|\tilde{z}|$. Letting $\tilde{z} = \sum_{i=1}^N \tilde{r}_i \exp[-j\frac{1}{2} k_c (t_i - \tau)^2]$ in Equation 4 and

carrying out the maximization yields the ML estimate of phase, $\hat{\theta}$, at any value of the delay τ :

$$\hat{\theta} = \arctan \left[\frac{\operatorname{Im} \left(\sum_{i=1}^N \tilde{r}_i \exp[-j\frac{1}{2} k_c (t_i - \tau)^2] \right)}{\operatorname{Re} \left(\sum_{i=1}^N \tilde{r}_i \exp[-j\frac{1}{2} k_c (t_i - \tau)^2] \right)} \right]. \quad (5)$$

Substituting this estimate into the simplified log-likelihood function $\Lambda_0(\tilde{\mathbf{r}} | \boldsymbol{\psi})$ maximizes it with respect to θ for any value of τ , yielding $|\tilde{z}|$, hence Equation 4 can be further simplified as follows:

$$\max_{\theta} \Lambda_0(\tilde{\mathbf{r}} | \Psi) = \left| \sum_{i=1}^N \tilde{r}_i \exp[-j \frac{1}{2} k_c (t_i - \tau)^2] \right|. \quad (6)$$

This last maximization can be accomplished by varying the delay τ over its uncertainty region, and selecting that value of delay, $\hat{\tau}$, that maximizes Equation 6.

The joint estimates of carrier phase and group delay can now be expressed as

$$(\hat{\theta}, \hat{\tau}) = \max_{\theta, \tau} \Lambda_0(\tilde{\mathbf{r}} | \Psi) = \max_{\tau} \left| \sum_{i=1}^N \tilde{r}_i \exp[-j \frac{1}{2} k_c (t_i - \tau)^2] \right|. \quad (7)$$

This operation is implemented by selecting a test delay τ' , multiplying the i -th received sample \tilde{r}_i by the i -th locally generated chirp signal sample corresponding to the test delay, $\exp[-j \frac{1}{2} k_c (t_i - \tau')^2]$, and evaluating the magnitude in Equation 7. This operation is repeated until the entire delay-uncertainty region $(\tau_{\min}, \tau_{\max})$, assumed to be known a priori, is covered with the desired delay-resolution, and the test-delay yielding the largest value selected as the optimal estimate of delay.

Note that if the phase θ is known a priori with great accuracy, $\hat{\theta} \equiv \theta$, then it can be removed from Equation 4 simply by pre-multiplying the complex argument of the conditional log-likelihood function by $\exp(j\hat{\theta})$, yielding

$$\Lambda_0(\tilde{\mathbf{r}} | \Psi)|_{\theta} = \text{Re} \left(\exp(j\hat{\theta}) \exp(-j\theta) \sum_{i=1}^N \tilde{r}_i \exp[-j \frac{1}{2} k_c (t_i - \tau)^2] \right) \equiv \text{Re} \left(\sum_{i=1}^N \tilde{r}_i \exp[-j \frac{1}{2} k_c (t_i - \tau)^2] \right)$$

as the function to be maximized. In other words, when the phase of the received signal is known, the delay estimate is obtained by varying the test delay τ' over the uncertainty region, computing the complex correlation between the received samples and the local reference over the entire chirp signal, taking the real part, and selecting that value of delay for which the log-likelihood function is the greatest:

$$\hat{\tau} = \max_{\tau} \Lambda_0(\tilde{\mathbf{r}} | \Psi)|_{\theta} = \max_{\tau} \text{Re} \left(\sum_{i=1}^N \tilde{r}_i \exp[-j \frac{1}{2} k_c (t_i - \tau)^2] \right). \quad (8)$$

The only difference in the estimation algorithms between the known phase and unknown phase case is that, with a known phase, the real part of the complex correlation is maximized, whereas with an unknown phase, the absolute value is maximized.

III. Cramer-Rao Bounds on the Variance of Phase and Delay Estimation

The variance of any unbiased estimator is lower bounded by the Cramer-Rao bound (CRB), which can be expressed in two distinct but equivalent forms: one involving the second derivative of the log-likelihood function, and another less familiar version using the square of the first derivative. As an illustrative example, estimation of delay (with all other

parameters known) would yield the following two equivalent forms for the CRB: the conventional form in Equation 9a, and the alternate form in Equation 9b.

$$\text{a) } \text{var}(\tau - \hat{\tau}) \geq \left(E \left[\frac{\partial^2 \Lambda(\mathbf{r} | \tau)}{\partial \tau^2} \right] \right)^{-1} \quad \text{and b) } \text{var}(\tau - \hat{\tau}) \geq \left(-E \left\{ \left[\frac{\partial \Lambda(\mathbf{r} | \tau)}{\partial \tau} \right]^2 \right\} \right)^{-1} \quad (9)$$

For the joint phase and delay estimation problem considered here, the CRB can be determined by evaluating the components of the Fisher information matrix,

$$\mathbf{I} = \begin{bmatrix} I_{11} & I_{12} \\ I_{21} & I_{22} \end{bmatrix}, \text{ where } I_{m,n} = -E \frac{\partial^2 \Lambda(\tilde{\mathbf{r}} | \boldsymbol{\Psi})}{\partial \psi_m \partial \psi_n} \quad m, n = 1, 2$$

and where $\psi_1 = \theta$ and $\psi_2 = \tau$, and E stands for the expectation operator. When neither parameter is known to the desired accuracy, so that joint estimation is required, the CRB for each component corresponds to the diagonal of the inverted Fisher information matrix, \mathbf{I}^{-1} .

If one of the parameters is assumed to be known, so that only one parameter needs to be estimated, then the CRB for this single-parameter case is given by the inverse of the corresponding diagonal elements of the diagonal Fisher information matrix:

I_{11}^{-1} for θ , and I_{22}^{-1} for τ . In other words, the diagonal elements represent the inverse of the CRB for the given parameter, assuming no coupling between parameters, or equivalently, assuming all other parameters are known and, hence, do not need to be estimated simultaneously.

We begin by evaluating the diagonal elements of the Fisher information matrix using the conventional second derivative of the log-likelihood function with respect to phase, I_{11} , and the second derivative of the log-likelihood function with respect to delay, I_{22} . The conditional log-likelihood function of Equation 4 is repeated here for convenience:

$$\Lambda_0(\tilde{\mathbf{r}} | \boldsymbol{\Psi}) = \text{Re} \left(\exp(-j\theta) \sum_{i=1}^N \tilde{r}_i \exp[-j \frac{1}{2} k_c (t_i - \tau)^2] \right). \quad (10)$$

A. Conventional Form of the CRB for Single-Parameter Phase Estimation

Carrying out the differentiation as indicated in Equation 9a, the first diagonal elements of the Fisher information matrix are

$$\begin{aligned}
I_{11} &= -E \frac{\partial^2 \Lambda(\tilde{\mathbf{r}} | \boldsymbol{\Psi})}{\partial \theta^2} = -E \left(\frac{2A}{\sigma_n^2} \frac{\partial}{\partial \theta} \operatorname{Re} \left(\frac{\partial}{\partial \theta} \exp(-j\theta) \sum_{i=1}^N \tilde{r}_i \exp[-j \frac{1}{2} k_c (t_i - \tau)^2] \right) \right) \\
&= -E \left(\frac{2A}{\sigma_n^2} \frac{\partial}{\partial \theta} \operatorname{Re} \left(-j \exp(-j\theta) \sum_{i=1}^N \tilde{r}_i \exp[-j \frac{1}{2} k_c (t_i - \tau)^2] \right) \right) \\
&= E \left(\frac{2A}{\sigma_n^2} \operatorname{Re} \left(\exp(-j\theta) \sum_{i=1}^N E \{ \tilde{r}_i \exp[-j \frac{1}{2} k_c (t_i - \tau)^2] \} \right) \right).
\end{aligned}$$

Substituting the received noise-corrupted samples $\tilde{r}_i = A \exp\{j \frac{1}{2} k_c (t_i - \tau)^2 + \theta\} + \tilde{n}_i$, and carrying out the expectation yields

$$\begin{aligned}
I_{11} &= \left(\frac{2A}{\sigma_n^2} \operatorname{Re} \left(E \sum_{i=1}^N \{ A \exp[j \frac{1}{2} k_c (t_i - \tau)^2 + \theta] + \tilde{n}_i \} \exp[-j \frac{1}{2} k_c (t_i - \tau)^2 + \theta] \right) \right) \\
&= \left(\frac{2A}{\sigma_n^2} \operatorname{Re} \left(\sum_{i=1}^N A + E(\tilde{n}_i) \exp[-j \frac{1}{2} k_c (t_i - \tau)^2 + \theta] \right) \right) = \frac{2NA^2}{\sigma_n^2} \quad \text{since } E(\tilde{n}_i) = 0.
\end{aligned}$$

If the delay is known, then the CRB for the variance of the phase estimation error is simply I_{11}^{-1} , hence the CRB on phase estimation for known delay becomes

$$\operatorname{var}(\theta - \hat{\theta}) \geq I_{11}^{-1} = \frac{\sigma_n^2}{2NA^2} = \frac{\sigma^2}{NA^2} \quad (11)$$

where $\sigma^2 = \sigma_n^2 / 2$ is the common variance of the real and imaginary components of the complex noise sample \tilde{n}_i .

B. Conventional Form of the CRB for Single-Parameter Delay Estimation

Proceeding as above, the second diagonal element of the Fisher information matrix can be determined as follows:

$$\begin{aligned}
I_{22} &= -E \frac{\partial^2 \Lambda(\tilde{\mathbf{r}} | \boldsymbol{\Psi})}{\partial \tau^2} = -E \frac{\partial}{\partial \tau} \left(\frac{2A}{\sigma_n^2} \operatorname{Re} \left(\exp(-j\theta) \sum_{i=1}^N \tilde{r}_i \frac{\partial}{\partial \tau} \exp[-\frac{1}{2} j k_c (t_i - \tau)^2] \right) \right) \\
&= E \left(\frac{2A}{\sigma_n^2} \operatorname{Re} \left(\exp(-j\theta) \sum_{i=1}^N \tilde{r}_i j \frac{\partial}{\partial \tau} k_c (t_i - \tau) \exp[-\frac{1}{2} j k_c (t_i - \tau)^2] \right) \right).
\end{aligned}$$

Carrying out the differentiation inside the sum yields

$$\begin{aligned}
j \frac{\partial}{\partial \tau} k_c (t_i - \tau) \exp[-\frac{1}{2} j k_c (t_i - \tau)^2] &= j \{ -k_c \exp[-\frac{1}{2} j k_c (t_i - \tau)^2] - j k_c^2 (t_i - \tau)^2 \exp[-\frac{1}{2} j k_c (t_i - \tau)^2] \} \\
&= -j k_c \exp[-\frac{1}{2} j k_c (t_i - \tau)^2] + k_c^2 (t_i - \tau)^2 \exp[-\frac{1}{2} j k_c (t_i - \tau)^2].
\end{aligned}$$

Substituting this expression into the sum, expanding the received samples into signal plus noise samples as before, $\tilde{r}_i = A \exp\{j\pi k_c(t_i - \tau)^2 + \theta\} + \tilde{n}_i$, and carrying out the expectation, yields

$$\begin{aligned}
I_{22} &= E \left(\frac{2A}{\sigma_n^2} \operatorname{Re} \left(\sum_{i=1}^N \tilde{r}_i j \frac{\partial}{\partial \tau} k_c(t_i - \tau) \exp[-j\{\frac{1}{2} k_c(t_i - \tau)^2 + j\theta\}] \right) \right) \\
&= E \left(\frac{2A}{\sigma_n^2} \operatorname{Re} \left(\sum_{i=1}^N \left(A \exp[j\{\frac{1}{2} k_c(t_i - \tau)^2 + \theta\}] + \tilde{n}_i \right) \right. \right. \\
&\quad \left. \left. \times \left(-jk_c \exp[-\frac{1}{2} jk_c(t_i - \tau)^2] + k_c^2(t_i - \tau)^2 \exp\{-j[\frac{1}{2} k_c(t_i - \tau)^2 + \theta]\} \right) \right) \right) \\
&= \frac{2A^2 k_c^2}{\sigma_n^2} \left(\sum_{i=1}^N (t_i - \tau)^2 \right).
\end{aligned} \tag{12}$$

Unlike the first diagonal element I_{11} , which is not a function of θ , the second diagonal element I_{22} depends on the delay τ . Letting $\Delta\tau = 1$ sample-interval for simplicity, so that $t_i = i\Delta\tau = i$, and expanding out the sum in Equation 12 yields

$$\sum_{i=1}^N (t_i - \tau)^2 = \sum_{i=1}^N (i^2 + \tau^2 - 2\tau i) = N\tau^2 + \sum_{i=1}^N i^2 - 2\tau \sum_{i=1}^N i = \frac{N(N+1)(2N+1)}{6} + N\tau^2 - \tau N(N+1).$$

Substituting this expression for the sum in Equation 12 yields the following equation for the second diagonal element:

$$I_{22} = \frac{2A^2 k_c^2}{\sigma_n^2} \left(\sum_{i=1}^N (i - \tau)^2 \right) = \frac{2A^2 k_c^2}{\sigma_n^2} \left(\frac{N(N+1)(2N+1)}{6} + N\tau^2 - \tau N(N+1) \right).$$

Therefore, with all other parameters known, the CRB for the delay estimate of a chirped signal becomes

$$\operatorname{var}(\tau - \hat{\tau}) \geq I_{22}^{-1} = \frac{\sigma_n^2}{2A^2 k_c^2} \left(\frac{N(N+1)(2N+1)}{6} + N\tau^2 - \tau N(N+1) \right)^{-1}. \tag{13}$$

Note that if the residual delay τ is small, such that $\tau^2 \ll N$, then the second and third terms inside the bracket of Equation 13 can be ignored, in which case Equation 13 simplifies to:

$$\operatorname{var}(\tau - \hat{\tau}) \underset{\tau \ll N}{\geq} \frac{\sigma_n^2}{2A^2 k_c^2} \left(\frac{N(N+1)(2N+1)}{6} \right)^{-1} \underset{N \rightarrow \infty}{\cong} \frac{\sigma_n^2}{A^2 k_c^2} \frac{3}{2N^3} = \frac{\sigma^2}{A^2 k_c^2} \frac{3}{N^3} \tag{14}$$

where $\sigma^2 = \sigma_n^2 / 2$ as before.

C. Alternate Form of CRB for Delay

For the problem of estimating the delay of a known signal observed in the presence of additive noise, the second form of the CRB shown in Equation 9b is often more

convenient, hence it will be used in the following derivation. Taking the derivative of the log-likelihood function with respect to the delay τ , yields

$$\frac{\partial}{\partial \tau} \Lambda(\mathbf{r} | \tau) = -\frac{1}{\sigma_n^2} \sum_{i=1}^N \frac{\partial}{\partial \tau} [r_i - s_i(t_i - \tau)]^2 = \frac{2}{\sigma_n^2} \sum_{i=1}^N [r_i - s_i(t_i - \tau)] \frac{\partial s_i(t_i - \tau)}{\partial \tau} = \frac{2}{\sigma_n^2} \sum_{i=1}^N n_i \frac{\partial s_i(t_i - \tau)}{\partial \tau}$$

where the last equality follows from the fact that $r_i - s_i(t_i - \tau) = n_i$. Substituting into Equation 9b, we obtain the following string of equations:

$$\begin{aligned} E \left\{ \left[\frac{\partial}{\partial \tau} \Lambda(\mathbf{r} | \tau) \right]^2 \right\} &= \frac{4}{\sigma_n^4} E \left\{ \left[\sum_{i=1}^N n_i \frac{\partial s_i(t_i - \tau)}{\partial \tau} \right]^2 \right\} \\ &= \frac{4}{\sigma_n^4} \left\{ \sigma_n^2 \sum_{i=1}^N \left[\frac{\partial s_i(t_i - \tau)}{\partial \tau} \right]^2 + \sum_{i=1}^N \sum_{\substack{j=1 \\ j \neq i}}^N E(n_i n_j) \frac{\partial s_i(t_i - \tau)}{\partial \tau} \frac{\partial s_j(t_j - \tau)}{\partial \tau} \right\} = \frac{4A^2}{\sigma_n^2} \sum_{i=1}^N \left[\frac{\partial s_i(t_i - \tau)}{\partial \tau} \right]^2 = {}_a I_{22} \end{aligned} \quad (15)$$

since $E(n_i n_j) = 0$ due to the assumed statistical independence of the noise samples.

Substituting into Equation 9a leads to the CRB for the error variance of any unbiased delay estimator:

$$\text{var}(\tau - \tau') \geq \left(E \left\{ \left[\frac{\partial}{\partial \tau} \Lambda(\mathbf{r} | \tau) \right]^2 \right\} \right)^{-1} = \frac{\sigma_n^2}{4A^2} \left(\sum_{i=1}^N \left[\frac{\partial s_i(t_i - \tau)}{\partial \tau} \right]^2 \right)^{-1}. \quad (16)$$

D. Conventional Form of CRB for Joint Estimation of Phase and Delay

Next, we compute the off-diagonal elements of the Fisher information matrix, I_{12} and I_{21} .

Carrying out the differentiation as above, we have the following derivation:

$$\begin{aligned} I_{12} &= -E \frac{\partial^2 \Lambda(\tilde{\mathbf{r}} | \boldsymbol{\Psi})}{\partial \theta \partial \tau} = -E \left(\frac{2A}{\sigma_n^2} \frac{\partial}{\partial \tau} \text{Re} \left(\frac{\partial}{\partial \theta} \exp(-j\theta) \sum_{i=1}^N \tilde{r}_i \exp[-j \frac{1}{2} k_c (t_i - \tau)^2] \right) \right) \\ &= -E \left(\frac{2A}{\sigma_n^2} \text{Re} \left(-j \exp(-j\theta) \sum_i \tilde{r}_i \frac{\partial}{\partial \tau} \exp[-j \frac{1}{2} k_c (t_i - \tau)^2] \right) \right) \\ &= E \left(\frac{2A}{\sigma_n^2} \text{Re} \left(j \exp(-j\theta) \sum_{i=1}^N j \tilde{r}_i k_c (t_i - \tau) \exp[-j \frac{1}{2} k_c (t_i - \tau)^2] \right) \right) \\ &= -\frac{2A}{\sigma_n^2} \text{Re} \left(\sum_{i=1}^N A k_c (t_i - \tau) + E \tilde{n}_i k_c (t_i - \tau) \exp[-j \frac{1}{2} k_c (t_i - \tau)^2 - j\theta] \right) \\ &= -\frac{2A^2 k_c}{\sigma_n^2} \sum_{i=1}^N (t_i - \tau) \rightarrow -\frac{2A^2 k_c}{\sigma_n^2} \frac{N(N+1)}{2} = -\frac{A^2 k_c}{\sigma_n^2} N(N+1). \end{aligned}$$

The inverse of the two-dimensional Fisher information matrix can be found by exchanging the diagonal components, changing the sign of the off-diagonal elements, and

dividing the resulting matrix by its determinant. With $\mathbf{I} = \begin{bmatrix} I_{11} & I_{12} \\ I_{21} & I_{22} \end{bmatrix}$ as above, the inverse of the Fisher information matrix is $\mathbf{I}^{-1} = \frac{1}{I_{22}I_{11} - I_{12}I_{21}} \begin{bmatrix} I_{22} & -I_{12} \\ -I_{21} & I_{11} \end{bmatrix}$.

The components of the Fisher information matrix are as follows:

$$I_{11} = \frac{2NA^2}{\sigma_n^2}, \quad I_{12} = I_{21} = -\frac{A^2k_c}{\sigma_n^2} N(N+1), \quad {}_c I_{22} = \frac{2A^2k_c^2}{\sigma_n^2} \left(\frac{N(N+1)(2N+1)}{6} \right) \text{ (conventional),}$$

assuming $\tau^2 \ll N$ as in Equation 14; and ${}_a I_{22} = \frac{A^2}{2\sigma_n^2} \sum_{i=0}^{N-1} \left[\frac{\partial s_i(iT_s - \tau)}{\partial \tau} \right]^2$ (alternate form).

Using the conventional form of the CRB, the products in the denominator are

$$I_{22}I_{11} = \frac{4NA^4k_c^2}{\sigma_n^4} \left(\frac{N(N+1)(2N+1)}{6} \right) = \frac{A^4k_c^2}{\sigma_n^4} \left(\frac{8N^4 + 12N^3 + 4N^2}{6} \right)$$

$$I_{12}I_{21} = \frac{A^4k_c^2}{\sigma_n^4} N^2(N+1)^2 = \frac{A^4k_c^2}{\sigma_n^4} \left(\frac{6N^4 + 12N^3 + 6N^2}{6} \right)$$

$$I_{22}I_{11} - I_{12}I_{21} = \frac{A^4k_c^2}{\sigma_n^4} \left(\frac{2N^4 - 2N^2}{6} \right) \underset{N \rightarrow \infty}{\cong} \frac{A^4k_c^2}{\sigma_n^4} \frac{N^4}{3}.$$

Substituting into the expression for the inverse of the Fisher information matrix yields the following expression:

$$\mathbf{I}^{-1} = \frac{1}{I_{22}I_{11} - I_{12}I_{21}} \begin{bmatrix} I_{22} & -I_{12} \\ -I_{21} & I_{11} \end{bmatrix} = \frac{3\sigma_n^4}{A^4N^4k_c^2} \begin{bmatrix} \frac{2A^2k_c^2}{\sigma_n^2} \frac{N^3}{3} & \frac{A^2k_c}{\sigma_n^2} N(N+1) \\ \frac{A^2k_c}{\sigma_n^2} N(N+1) & \frac{2NA^2}{\sigma_n^2} \end{bmatrix}.$$

The CRBs for joint delay and phase estimation are the diagonal elements of \mathbf{I}^{-1} :

$$\text{var}(\theta - \hat{\theta})_{\tau, \theta} \geq \frac{3\sigma_n^4}{A^4N^4k_c^2} \frac{2A^2k_c^2}{\sigma_n^2} \frac{N^3}{3} = \frac{2\sigma_n^2}{NA^2} = \frac{4\sigma^2}{NA^2} \quad (17)$$

$$\text{var}(\tau - \hat{\tau})_{\tau, \theta} \geq \frac{3\sigma_n^4}{A^4N^4k_c^2} \frac{2NA^2}{\sigma_n^2} = \frac{6\sigma_n^2}{A^2N^3k_c^2} = \frac{12\sigma^2}{A^2N^3k_c^2} \quad (18)$$

In order to establish their validity, the above CRBs for single-parameter and joint estimation of phase and delay are compared to simulation results in the next section.

IV. Simulation and Numerical Results

After downconversion to complex baseband, the chirp signal can be represented in terms of real and imaginary components as shown in Figure 1, where the solid blue curve is the real part and the dashed blue curve is the imaginary part of the chirp reference signal, respectively. This chirp signal was generated in MATLAB, along with the delay estimator algorithms defined in Equations 7 and 8. Both reference signals and noisy delayed received echo signals were simulated, and input to the ML estimator for processing.

The delayed noisy received echo can be similarly represented in terms of real and imaginary components: the relationship between the reference and received noisy signals can be seen in terms of their respective real parts in Figure 2, where a fractional symbol delay of 53 samples was applied to the received symbol, as an example.

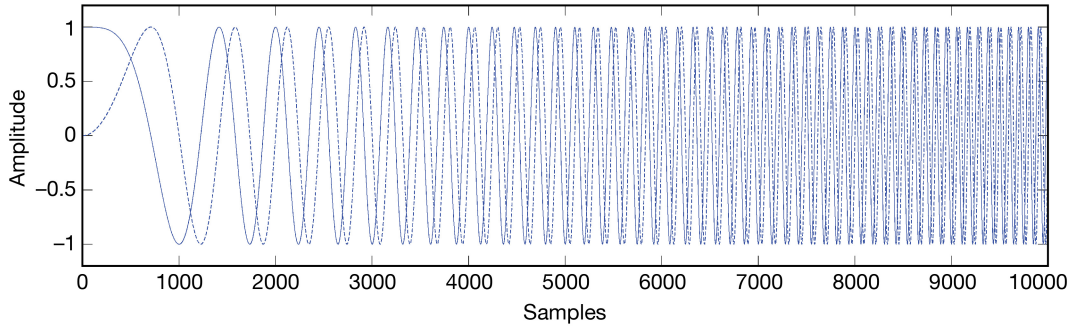


Figure 1. Example of real (solid) and imaginary (dashed) components of the chirp reference signal.

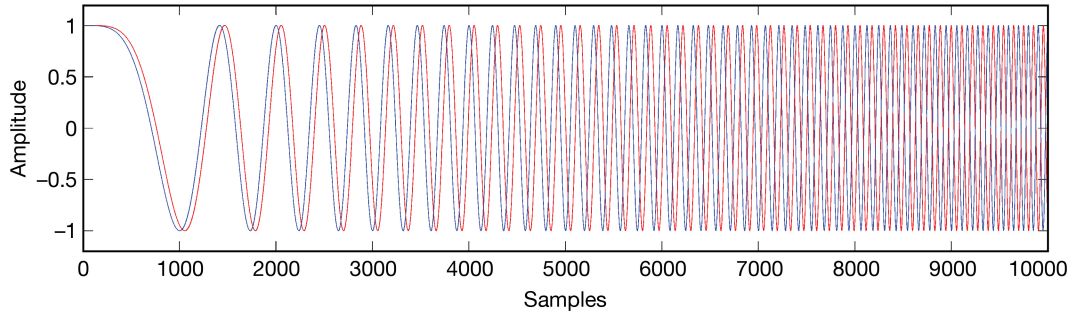


Figure 2. Example of real part of reference chirp signal (blue) and real part of the delayed received chirp signal (red), with 53 sample delay applied.

A. Single-Parameter CRB

We consider the single-parameter estimation of delay and phase first, where the CRB for each parameter is the diagonal element of the Fisher information matrix. The CRB for phase estimation error is given by Equation 11, repeated here for convenience:

$$\text{var}(\theta - \hat{\theta}) \geq I_{11}^{-1} = \frac{\sigma_n^2}{2NA^2} = \frac{\sigma^2}{NA^2}.$$

Two distinct forms of the CRB have been derived for delay estimation, termed “conventional” and “alternate:”

$$\text{Conventional: } \text{var}(\tau - \hat{\tau}) \geq \frac{\sigma^2}{A^2 k_c^2} \frac{3}{N^3}; \quad \text{Alternate: } \text{var}(\tau - \hat{\tau}) \geq \frac{\sigma^2}{2} \left(\sum_{i=0}^{N-1} \left[\frac{\partial s_i(iT_s - \tau)}{\partial \tau} \right]^2 \right)^{-1}.$$

The alternate form of the CRB relies on the derivative of the reference signal, which can be computed numerically when the reference signal is known. As an example, the I and Q components of the derivative of the chirp reference signal are shown in Figure 3 (solid and dashed green curves), with the magnitude shown as the envelope (blue line).

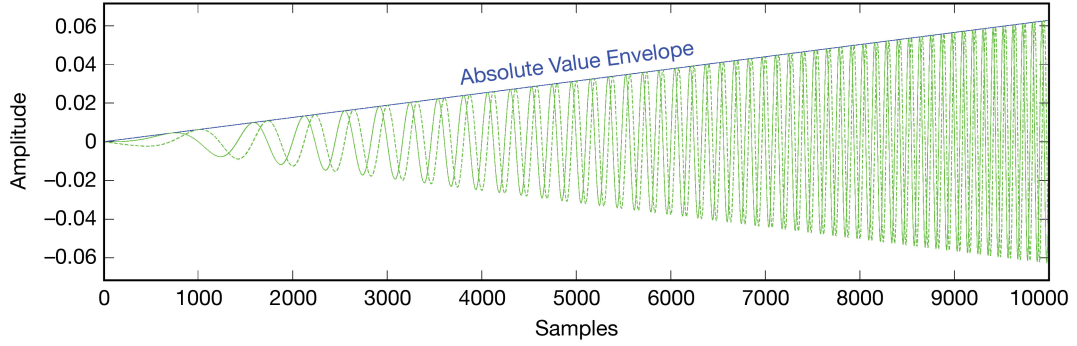


Figure 3. Derivative of real and imaginary parts (green solid and dashed curves, respectively) of reference signal, and absolute value (blue line) used in the alternate form of the CRB in Equation 19.

The CRB for the joint estimation of phase and delay are given by Equations 17 and 18, respectively, using the conventional form of the CRB and repeated here for convenience:

$$\text{var}(\theta - \hat{\theta})_{\tau, \theta} \geq \frac{4\sigma^2}{NA^2} \quad \text{var}(\tau - \hat{\tau})_{\tau, \theta} \geq \frac{12\sigma^2}{A^2 N^3 k_c^2}.$$

Note that joint estimation incurs a penalty of a factor of 4, or 6 dB in error variance, as can be seen in Figures 5 and 9 by the black dashed lines representing the CRB for phase and delay.

B. Delay Estimation

The ML delay estimation algorithms for simultaneous estimation of carrier phase and pulse delay were implemented in MATLAB, and used to generate simulated delay estimates with chirp signals as input. Delay was computed as the difference between the index of the peak of the reference and auto-correlation functions, an example of which is shown in Figure 4 using a delay of 53 samples at high sample-SNR. As can be seen in Figures 1-3, 10^4 samples were used per chirp pulse, and chirp parameters of 6×10^{-6} Hz/sample, or equivalently $2\pi(6 \times 10^{-6})$ radians/sample were employed in the simulations.

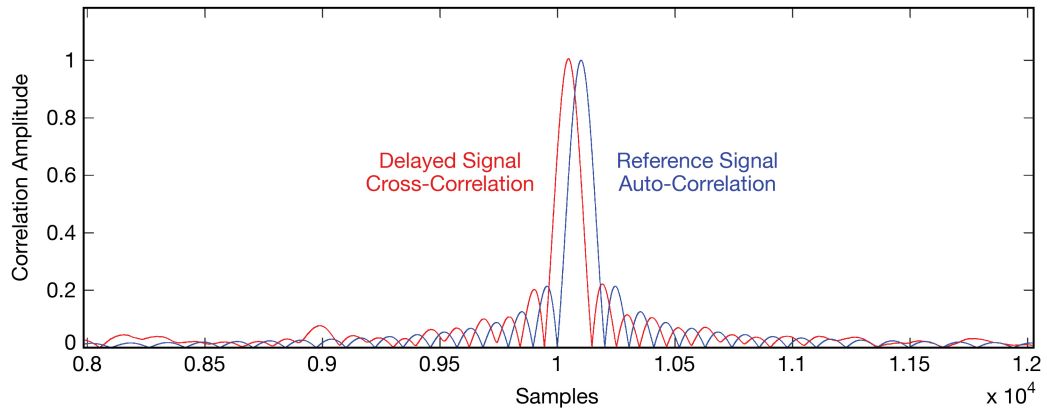


Figure 4. Auto-correlation function of reference signal (blue), and cross-correlation of reference-received signal (red). The delay estimate is determined by differencing the indices of the peaks.

The results of the delay estimation algorithm are shown in Figure 5. The blue asterisks are the simulated performance of the single-parameter delay estimator, whereas the black asterisks are the simulated performance of the joint delay-phase estimator. Note that a root mean square (rms) delay error of 0.1 sample can be achieved with a sample-SNR of approximately -5 dB when the phase is known, but $+1$ dB is required when joint estimates are used.

The conventional form of the CRB given in Equation 14 is shown as the dashed red line in Figure 5, verifying the equivalence of the two forms of the CRB. The alternate form of the CRB in Equation 16 was also computed to validate the simulation results, and shown in the performance plot of Figure 5 as the dashed blue line superimposed on the dashed red line, showing equivalence of these two expressions. The conventional form of Equation 14 employs signal parameters, including the chirp parameter k_c , the number of samples N , signal amplitude A , and the sample noise variance used to calculate sample-SNR; hence, a complete mathematical description is required. The alternate form of the CRB does not require a complete mathematical description, relying instead on the energy in the derivative of the signal, hence it can be computed from a measured waveform even if a precise mathematical description is not available.

Three distinct regions can be identified in Figure 5, with notably different characteristics: a high-SNR region where the estimators approach the CRB for the single-parameter case; a medium-SNR region where the estimators begin to deviate from the CRB; and a low-SNR region where a rapid increase in estimation error occurs, effectively rendering these estimates unusable.

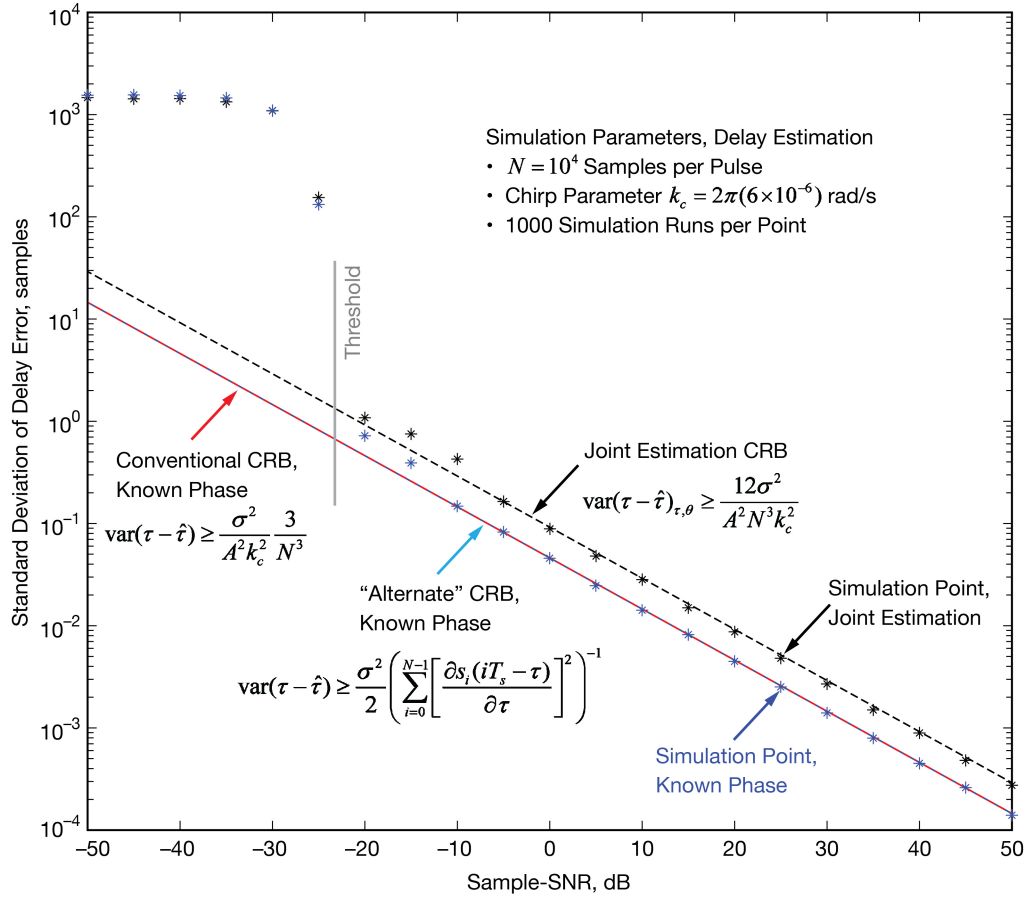


Figure 5. CRB and simulation results for single-parameter delay (red and blue dashed line and blue asterisks), and simultaneous phase-delay estimates (black dashed line and black asterisks).

1. High-SNR region

In the high-SNR region, nominally greater than -10 dB, the rms delay errors are much less than 1, in other words, much smaller than the sample-interval. The delay estimates tend to be close to the integer input sample delay, resulting in apparently zero delay error even with a large number of simulations per delay estimate, when the estimates are restricted to be integer samples. A quadratic interpolation algorithm was therefore developed using the location and value of the correlation peak and its two nearest neighbors, to refine the delay estimates to a small fraction of a sample.

Figure 6 shows the chirp correlation functions near the peaks, and the interpolation algorithm for a delay of 13 samples in the high-SNR region. Figure 6a) is a zoomed version of the correlation peaks, showing the two peaks separated by the integer input sample delay. It can be seen in Figure 6b) that the interpolated peaks (black circles) between the peak sample and its two nearest neighbors (red asterisks) are close to, but not exactly equal to the raw sample peaks. The true delay variance can now be estimated with a reasonable number of simulations per point, even in the high-SNR region.

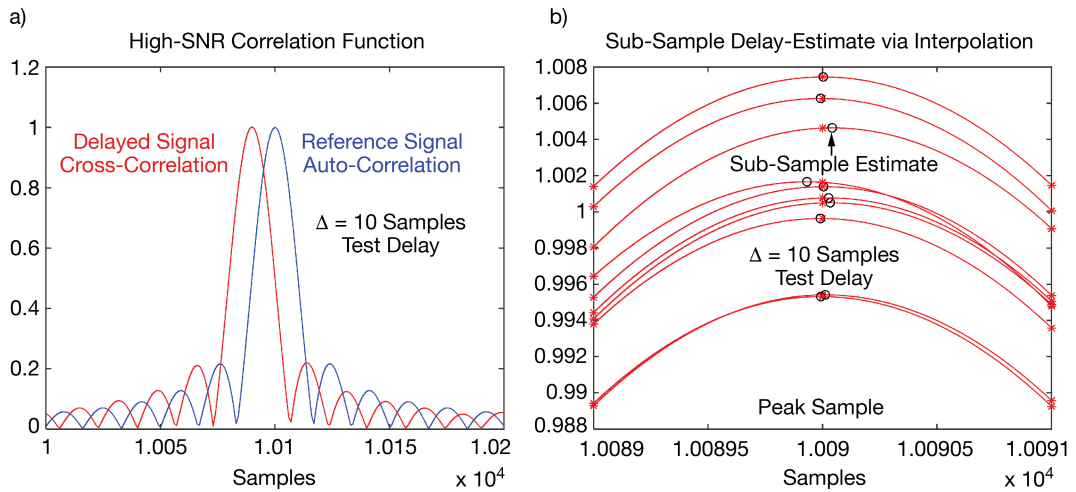


Figure 6. Correlation functions and fine delay estimates in the high-SNR regime.

2. Medium-SNR region

The slight increase in rms delay error over the CRB in the intermediate or “medium SNR” region between -25 dB and -10 dB seen in Figure 5 can be understood by referring to Figure 7. The zoomed correlation peaks in Figure 7a) show an increased impact of noise on the cross-correlation peak, leading to increased errors in the interpolated estimates, including occasional sample-level errors, as shown in Figure 7b). These occasional sample errors tend to increase the measured errors slightly above the CRB, as shown in Figure 5.

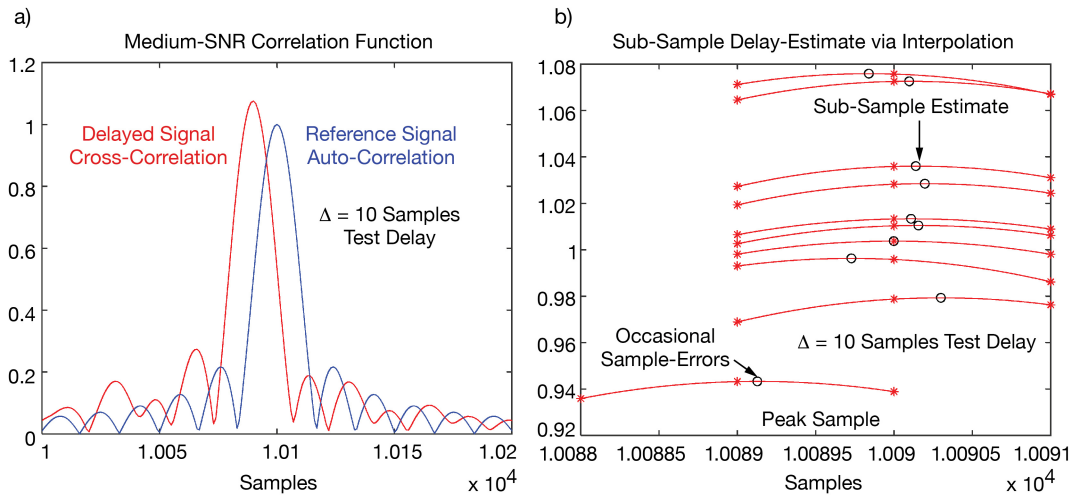


Figure 7. Correlation functions and fine delay estimates in the mid-SNR region.

3. Low-SNR region

Outliers begin to occur when the sample-SNR dips below -25 dB, causing a sudden increase in delay estimation error below the threshold. This effect is due to large noise spikes that exceed the cross-correlation peak and can occur anywhere within the delay uncertainty range, as can be seen in Figure 8a, where the largest cross-correlation peak is about 300 samples from the true delay. Even a few of these large outlier spikes can increase the variance estimate significantly, leading to the nonlinear behavior in the low-SNR region

(below -25 dB) shown in Figure 5. Since the interpolation algorithm works at the cross-correlation peak, it cannot reduce large integer-sample errors caused by outliers; hence, it is not effective below the threshold and cannot prevent large errors in this region.

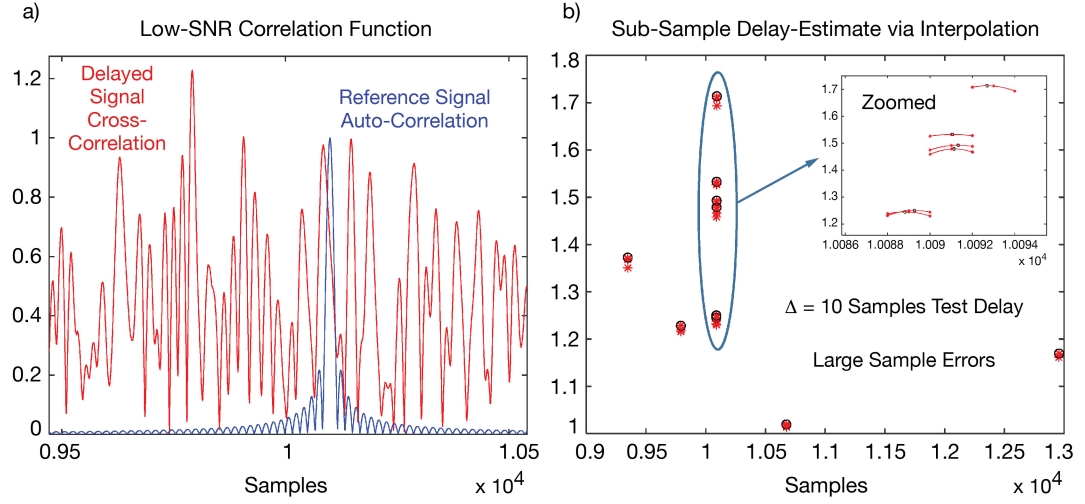


Figure 8. Correlation functions and fine delay estimates in the low-SNR region.

C. Phase Estimation

The performance of the phase estimation algorithm for the single-parameter estimates of Equation 11 and those obtained from the joint phase-delay estimator of Equation 17, are shown in Figure 9. The single-parameter estimates are obtained in the simulation by taking the arc-tangent of the ratio of the imaginary part to the real part of the cross-correlation between the received signal and the reference, at the known delay, τ_0 :

$$\hat{\theta} = \arctan \left[\frac{\text{Im} \left(\sum_{i=1}^N \tilde{r}_i \exp[-j \frac{1}{2} k_c (t_i - \tau_0)^2] \right)}{\text{Re} \left(\sum_{i=1}^N \tilde{r}_i \exp[-j \frac{1}{2} k_c (t_i - \tau_0)^2] \right)} \right]. \quad (19)$$

The results are shown in Figure 9 as the blue asterisks, virtually superimposed on the CRB for the known delay case given by Equation 11, above a sample-SNR of -20 dB. In the simulation, 10^4 samples were used per chirp pulse, and the chirp rate was set to 6×10^{-6} Hz/sample as before. Note that the phase estimates also exhibit thresholding below a sample-SNR of -25 dB, similar to the delay estimates shown in Figure 5, with a maximum standard deviation of approximately 2 radians.

When the delay is not known, the phase and delay must be estimated simultaneously according to Equation 17. The resulting estimates are shown as black asterisks in Figure 9, again in excellent agreement with the CRB for joint phase-delay estimates given by Equation 17. It can be seen that phase estimates of approximately one tenth of a radian can be achieved with a sample-SNR of -20 dB when the delay is known, and roughly -14 dB with joint estimation, when the chirp pulses are sampled at a rate of 10^4 samples/pulse.

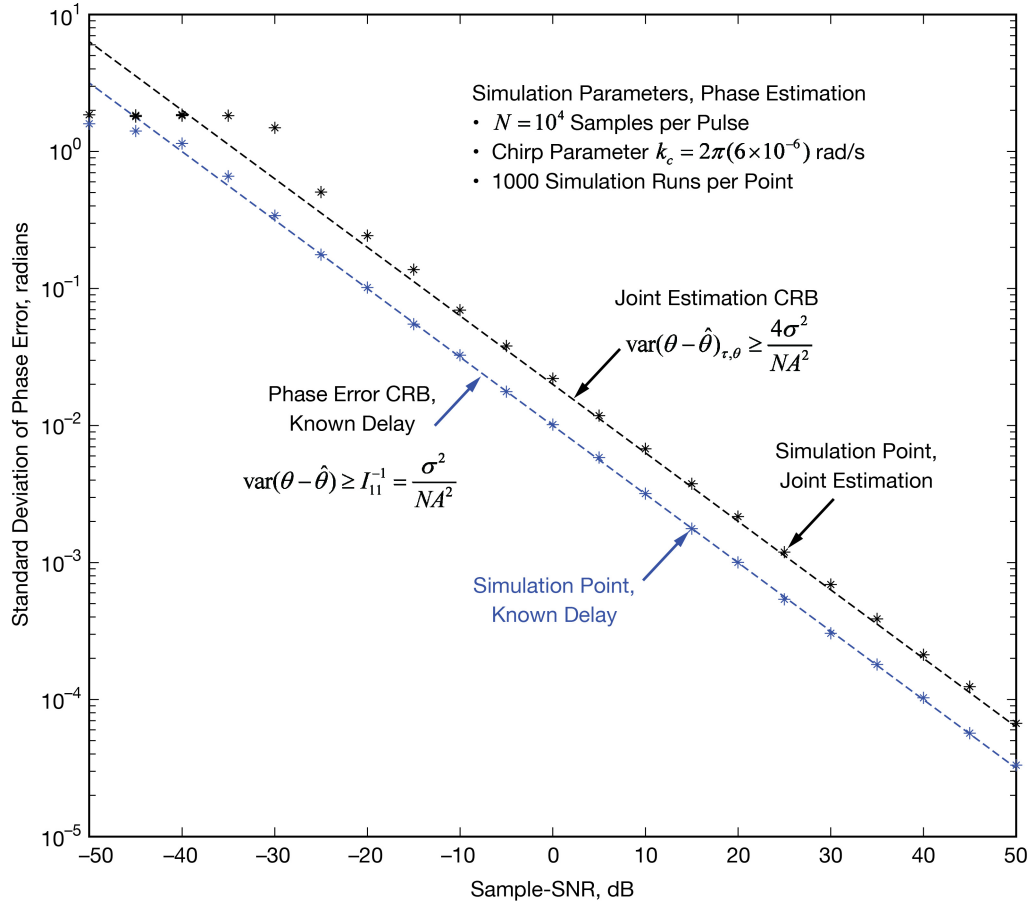


Figure 9. CRB and simulation results for single-parameter phase (blue dashed line and asterisks), and simultaneous phase-delay estimates (black dashed line and asterisks).

The results for carrier phase and delay estimation error shown in Figures 4 and 9 can be converted to familiar engineering units by considering a specific sampling rate in terms of samples per second. As an example, consider a sampling rate of 10^6 samples per second, yielding a total integration time of 0.01 second, or 10 milliseconds, for a chirped pulse with 10^4 samples per pulse. Reading directly from Figure 9, it can be seen that, with joint estimation, carrier phase can be estimated with an rms error of 0.1 radian at a sample-SNR of approximately -14 dB. Using a factor of 10^4 , or 40 dB, to convert sample-SNR to pulse-SNR, it follows that 26 db of pulse-SNR is required to achieve 0.1 radian phase error with joint estimation. Similarly, from Figure 4, it can be seen that this would result in a delay estimation error of less than 1 sample on the average, which may be adequate for group-delay in many applications. The required integration times are in fact so short that continuous calibration, or tracking of the array phase may be possible with roughly 10 millisecond updates, potentially enabling real-time compensation for tropospheric fluctuations that could degrade phased array performance at microwave frequencies.

V. Summary and Conclusions

The application of chirped signals to phased array calibration was addressed in this paper, incorporating the concept of joint estimation of carrier phase and pulse delay. The structure of the ML estimators was derived, and their performance evaluated via simulation under a wide range of SNRs. The CRBs on estimator performance were also derived and used to validate the simulation results. It was found that the joint estimator performs close to the CRB at high SNRs, but begins to degrade and eventually fail at very low sample-SNR, as expected. Three distinct SNR regions were identified and analyzed to explain estimator behavior at low, medium, and high SNR. It was shown that the proposed estimator structure enables rapid calibration and even continuous tracking of array phase and group delay, enabling real-time compensation for tropospheric fluctuations in addition to initial calibration of phased arrays, under conditions typical of DSN operations.

References

- [1] M. A. Slade, L. A. M. Benner, and A. Silva, "Goldstone Solar System Radar Observatory: Earth-Based Planetary Mission Support and Unique Science Results," *Proc. IEEE 0012-9219*, 2010.
- [2] V. Vilnrotter, D. Lee, P. Tsao, T. Cornish, and L. Paal, "Uplink Array Calibration via Lunar Doppler-Delay Imaging," *Proceedings of the IEEE Aerospace Conference*, Big Sky, MN, 2010.
- [3] V. Vilnrotter, P. Tsao, D. Lee, T. Cornish, J. Jao, M. Slade, "Planetary Radar Imaging with the Deep-Space Network's 34 meter Uplink Array," *Proceedings of the IEEE Aerospace Conference*, Big Sky, MN, 2011, vol. 2, pp.1283-1290.
- [4] V. A. Vilnrotter, P. C. Tsao, D. K. Lee, T. P. Cornish, L. Paal, J. Vahraz, "Uplink Array Concept Demonstration with the EPOXI Spacecraft," *IEEE Aerospace and Electronic Systems Magazine*, vol. 15, no. 5, 2010.